

Effect of poly (l-lactic acid) scaffolds seeded with aligned diaphragmatic myoblasts overexpressing connexin-43 on infarct size and ventricular function in sheep with acute coronary occlusion

Carlos Sebastián Giménez, Fernanda Daniela Olea, Paola Locatelli, Ricardo A. Dewey, Gustavo Abel Abraham, Florencia Montini Ballarin, Maria del Rosario Bauzá, Anna Hnatiuk, Andrea De Lorenzi, Ángela Neira Sepúlveda, Mario Embon, Luis Cuniberti & Alberto Crottogini

To cite this article: Carlos Sebastián Giménez, Fernanda Daniela Olea, Paola Locatelli, Ricardo A. Dewey, Gustavo Abel Abraham, Florencia Montini Ballarin, Maria del Rosario Bauzá, Anna Hnatiuk, Andrea De Lorenzi, Ángela Neira Sepúlveda, Mario Embon, Luis Cuniberti & Alberto Crottogini (2018): Effect of poly (l-lactic acid) scaffolds seeded with aligned diaphragmatic myoblasts overexpressing connexin-43 on infarct size and ventricular function in sheep with acute coronary occlusion, *Artificial Cells, Nanomedicine, and Biotechnology*, DOI: [10.1080/21691401.2018.1508029](https://doi.org/10.1080/21691401.2018.1508029)

To link to this article: <https://doi.org/10.1080/21691401.2018.1508029>



Published online: 05 Oct 2018.




Submit your article to this journal [↗](#)



View Crossmark data [↗](#)



Effect of poly (l-lactic acid) scaffolds seeded with aligned diaphragmatic myoblasts overexpressing connexin-43 on infarct size and ventricular function in sheep with acute coronary occlusion

Carlos Sebastián Giménez^a , Fernanda Daniela Olea^a, Paola Locatelli^a, Ricardo A. Dewey^b, Gustavo Abel Abraham^c, Florencia Montini Ballarin^c, Maria del Rosario Bauzá^a, Anna Hnatiuk^a, Andrea De Lorenzi^d, Ángela Neira Sepúlveda^d, Mario Embon^d, Luis Cuniberti^a and Alberto Crottogini^a

^aInstituto de Medicina Traslacional, Trasplante y Bioingeniería (IMETTYB), Universidad Favaloro-CONICET, Buenos Aires, Argentina; ^bInstituto de Investigaciones Biotecnológicas-Instituto Tecnológico de Chascomús (IIB-INTECH), Universidad Nacional de San Martín-CONICET, Chascomús, Argentina; ^cInstituto de Investigaciones en Ciencia y Tecnología de Materiales (INTEMA), Universidad Nacional de Mar del Plata-CONICET, Mar del Plata, Argentina; ^dHospital Universitario de la Fundación Favaloro, Buenos Aires, Argentina

ABSTRACT

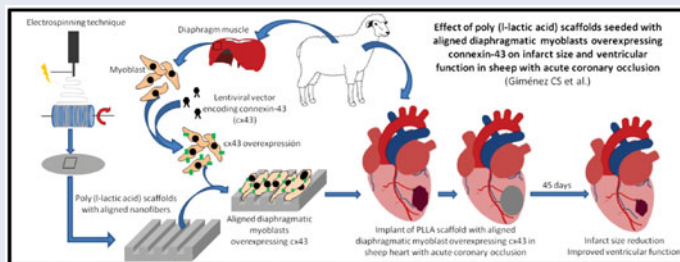
Diaphragmatic myoblasts (DM) are stem cells of the diaphragm, a muscle displaying high resistance to stress and exhaustion. We hypothesized that DM modified to overexpress connexin-43 (cx43), seeded on aligned poly (l-lactic acid) (PLLA) sheets would decrease infarct size and improve ventricular function in sheep with acute myocardial infarction (AMI). Sheep with AMI received PLLA sheets without DM (PLLA group), sheets with DM (PLLA-DM group), sheets with DM overexpressing cx43 (PLLA-DMcx43) or no treatment (control group, $n=6$ per group). Infarct size (cardiac magnetic resonance) decreased ~25% in PLLA-DMcx43 [from 8.2 ± 0.6 ml (day 2) to 6.5 ± 0.7 ml (day 45), $p < .01$, ANOVA-Bonferroni] but not in the other groups. Ejection fraction (EF%) (echocardiography) at 3 days post-AMI fell significantly in all groups. At 45 days, PLLA-DM y PLLA-DMcx43 recovered their EF% to pre-AMI values (PLLA-DM: $61.1 \pm 0.5\%$ vs. $58.9 \pm 3.3\%$, $p = \text{NS}$; PLLA-DMcx43: $64.6 \pm 2.9\%$ vs. $56.9 \pm 2.4\%$, $p = \text{NS}$), but not in control ($56.8 \pm 2.0\%$ vs. $43.8 \pm 1.1\%$, $p < .01$) and PLLA ($65.7 \pm 2.1\%$ vs. $56.6 \pm 4.8\%$, $p < .01$). Capillary density was higher ($p < .05$) in PLLA-DMcx43 group than in the remaining groups. In conclusion, PLLA-DMcx43 reduces infarct size in sheep with AMI. PLLA-DMcx43 and PLLA-DM improve ventricular function similarly. Given its safety and feasibility, this novel approach may prove beneficial in the clinic.

ARTICLE HISTORY

Received 27 June 2018
Revised 27 July 2018
Accepted 27 July 2018

KEYWORDS

acute myocardial infarction; diaphragmatic myoblasts; connexin-43; poly (l-lactic acid); scaffolds; regenerative medicine



Introduction

Ischemic heart disease is the main cause of mortality worldwide [1]. Its complication, acute myocardial infarction (AMI), leads to progressive replacement of the remaining contractile tissue by fibrosis, a process known as ventricular remodeling which, in turn, leads to heart failure [2]. It has been shown that the extent of remodeling and thus the severity of heart failure largely depend on infarct size [3–5]. In this regard, cardiac regenerative therapies employing stem cells and tissue engineering can potentially reduce infarct size and improve left ventricular (LV) function [6].

Skeletal myoblasts (SkM) are an attractive cell type for cardiomyoplasty as they have a contractile phenotype, can be

easily harvested, are resistant to ischemia and secrete cytokines and growth factors involved in cardiac repairing routes [7,8]

Although it has been reported that SkM exhibit differences depending on the muscle from where they are obtained, this fact has not been taken into account for designing these therapies [9,10]. In this regard, diaphragmatic myoblasts (DM) may be suitable for myocardial regeneration for they are precursors of type 1 fibers and display a much higher exhaustion threshold than other muscles, on account that they contract and relax 20 times per minute over a lifetime.

As cardiac synchronous contraction depends on the propagation of the action potentials through the syncytium,

it is necessary to stimulate inter-cellular connections of the cells to be implanted. We have recently shown that DM modified to overexpress cx43 and seeded on aligned nanofibers of poly (l-lactic acid) (PLLA) that mimic the topography of cells in skeletal muscle increased inter-cellular connectivity *in vitro* [11]. However, whether or not this approach affords cardioprotection *in vivo* remains to be demonstrated. We thus aimed at assessing the effect of the implant of aligned DM overexpressing cx43 seeded on PLLA scaffolds on infarct size and LV function in a sheep model of AMI.

Materials and methods

All procedures were performed in accordance with the Guide for Care and Use of Laboratory Animals (NIH Publication No. 85–23, revised 1996) and approved by the Laboratory Animal Care and Use Committee (CICUAL) of the Favaloro University (approval #DCT0153-12).

DM preparation

Obtention, processing and transduction of ovine DM have been reported previously [11]. Briefly, a sterile right mini-thoracotomy was performed in the 6th intercostal space under general anesthesia to obtain a diaphragm biopsy (~2 cm²). DM were isolated, cultured and genetically modified with a lentiviral vector (Lv.pCMV/CX43iresGFP) to overexpress cx43 and green fluorescence protein (GFP).

Scaffolds preparation

Four days before experimental AMI surgery, PLLA scaffolds of 5.5 cm in diameter were hydrated with PBS buffer (Gibco, Grand Island, NY) and cultured with 1×10^7 DM or DMcx43 at 37 °C and 5% CO₂ in high-glucose Dulbecco's modified Eagle medium (DMEM, Gibco) supplemented with 2% (v/v) antibiotic-antimycotic (Anti-Anti, Gibco), 20% (v/v) fetal bovine serum (Natacor, Buenos Aires, Argentina), for the PLLA-DM and PLLA-DMcx43 groups, respectively. In this step, surgical steel rings designed in our laboratory were used to simulate culture plates with PLLA polymer as culture surfaces (supplementary Figure 1). With this method, possible variations in the therapeutic cell dose by cell leak were prevented. After 4 d, the cells became adhered and aligned on the scaffold.

Ovine model of AMI

Male Corriedale sheep, weighting 31.3 ± 4.6 kg were premedicated with intramuscular acepromazine maleate 5 mg (Holliday-Scott, Beccar, Argentina). Anesthesia was induced with intravenous propofol 3 mg/kg and maintained with 2% isoflurane in oxygen using mechanical ventilation.

Under electrocardiographic and pulse oximetry monitoring, a sterile thoracotomy was performed at the 4th intercostal space and an anterior-apical infarct (~20% of the LV mass) was induced by permanent ligation of branches of the left anterior descending artery (LAD), avoiding the first diagonal branch (Figure 1(A)). The LAD itself was not ligated to

prevent septal infarction. To reduce the incidence of ventricular arrhythmias, lidocaine (3 intravenous boluses of 1 mg/kg followed by 2 mg/kg in saline infusion) and amiodarone (150 mg in saline infusion) were administered until the end of surgery. Forty minutes after ligation, sheep were randomly distributed to receive a PLLA scaffold without cells (PLLA group, $n = 6$), a PLLA scaffold seeded with DM (PLLA-DM group, $n = 6$), a PLLA scaffold seeded with DM overexpressing cx43 (PLLA-DMcx43 group, $n = 6$), or no treatment (control group, $n = 6$). The scaffold border was sutured to the myocardium with prolene 5–0 (Ethicon Inc., NJ) in four to seven equidistant points, covering the infarcted area and ~1 cm of its periphery (Figure 1(B) and supplementary video). Finally, the thoracotomy was closed and the endotracheal tube was removed. Intravenous cefazolin 1 g was administered and the animal was returned to the animal house under analgesic treatment (subcutaneous nalbuphine 0.3 mg/kg).

Cardiac magnetic resonance (CMR)

Two and 45 d post-infarction, CMR (1.5 Tesla scanner, Achieva, Philips, Amsterdam, The Netherlands) was performed to measure infarct size. Ten short-axis slices spanning the heart from apex to base and measuring 8 mm in thickness were acquired without gaps. Gadolinium-based contrast 0.2 mmol/kg (Dotarem, Temis Lostaló, Buenos Aires, Argentina) was administered, and delayed contrast-enhanced images were acquired with a phase-sensitive inversion recovery sequence (PSIR) starting 8 min after contrast injection. Image data for each animal were combined, anonymised and analysed with a semiautomated segmentation method using freely available software (Segment, version 1.8 R1172; <http://segment.heiberg.se>). Infarct size was expressed as milliliters of infarcted tissue.

Echocardiography

Bidimensional echocardiography (Sonos 5500, Hewlett-Packard, Palo Alto, CA) was performed under light sedation (diazepam 10 mg intravenous) with the animal laying on its right lateral decubitus using 2.5–4 MHz transducers. Parasternal long- and short-axis views were recorded 2 d before AMI and at 3 and 45 d post-AMI. End-diastolic and end-systolic volumes (EDV and ESV, respectively) were measured by single-plane multiple overlapped disks method and LV ejection fraction (EF%) was calculated as $(EDV - ESV) / EDV \times 100$.

It should be noted that biplane methods could not be applied, as in sheep, it is not possible to obtain truly orthogonal views from the parasternal window. We have previously shown that echocardiographic parameters of systolic and diastolic LV performance in young adult sheep can be reliably extrapolated to the adult human [12].

Histological and gene expression analyses

After completing their respective protocols, sheep were premedicated with intramuscular acepromazine maleate (10 mg total) and euthanized with a propofol overdose

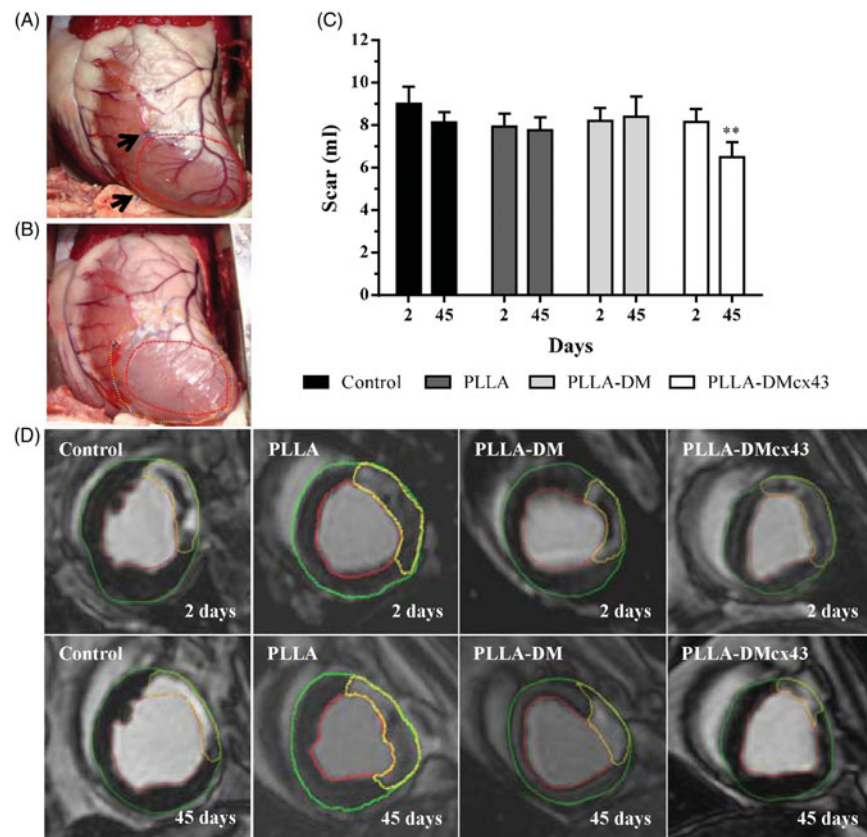


Figure 1. Surgical procedure and infarct size. (A) Induction of a left ventricular antero-apical infarct by occlusion of two branches of the left anterior descending artery; arrows indicate the ligatures and the red dotted line the ischemic region. (B) PLLA scaffold (yellow dotted line) implanted on the infarct and adjacent non infarcted myocardium (C) Infarct size measured by cardiac magnetic resonance at 2 and 45 d post-AMI and expressed as ml of scar tissue. Significant infarct size reduction occurs only in the PLLA-DMcx43 group (** $p < .01$ vs. day 2, mean \pm SEM, two-way ANOVA, Bonferroni) (D) Representative LV short axis cardiac magnetic resonance images with late gadolinium enhancement acquired at end diastole at 2 and 45 d post-AMI in an animal of each group. In all images the infarct is delineated in yellow, the epicardium in green and the endocardium in red. The animal belonging to the PLLA-DMcx43 group exhibits the largest reduction in infarct size. PLLA: poly(l)lactic acid (PLLA) scaffold devoid of cells; PLLA-DM: PLLA scaffold seeded with diaphragmatic myoblasts (DM); PLLA-DMcx43: PLLA scaffold seeded with DM overexpressing connexin-43 (cx43).

(13–20 mg/kg) followed by potassium chloride (60 mEq) to arrest the heart in diastole. The heart was extracted and samples of the infarct and peri-infarct regions were harvested for histological and gene expression analyses. Histological analysis comprised quantification of fibrosis, measurement of microvascular density and detection of the biomaterial. Expression of angiogenic genes (VEGF, angiogenin, PGF) and cardiac lineage precursor genes (Nkx 2.5, GATA-4, C-Kit) was assessed by real-time PCR. The detailed methodology is described in on-line [Supplementary material](#).

Statistical analysis

Variables were analyzed with 1-way ANOVA-Bonferroni for intergroup comparisons or 2-way ANOVA, Bonferroni for inter- and intra-group comparisons, using GraphPad Prism software (version 5.0; GraphPad Software Inc., La Jolla, CA). Statistical significance was set at $p < .05$. Results are expressed as mean \pm SEM.

Results

Animal loss

Twenty-four sheep were operated. One animal from the PLLA group died due to irreversible ventricular fibrillation 2 d after

AMI. This animal was replaced to complete $n = 6$ in that group.

Infarct size

Two days post-treatment infarct size was similar among groups. Paired analysis revealed that from days 2 to 45 post-occlusion, infarct size decreased significantly in the PLLA-DMcx43 group (8.2 ± 0.6 vs. 6.5 ± 0.7 ml, $p < .01$), but not in the other groups (control: 9.0 ± 0.8 vs. 8.1 ± 0.5 ml; PLLA: 7.9 ± 0.6 vs. 7.8 ± 0.5 ml; PLLA-DM: 8.2 ± 0.6 vs. 8.4 ± 0.9 ml; all $p = \text{NS}$) (Figure 1(C)).

Figure 1(D) shows representative CMR LV short-axis slices for each experimental group at 2 and 45 d post-AMI.

Cardiac function

Figure 2(A) shows EF% and LV volumes at baseline (day 3) and at 3 and 45 d post-AMI. At baseline, EF% was similar among groups, and decreased at 3 d post-AMI (control: 56.8 ± 2 vs. $38.4 \pm 2.9\%$, $p < .01$; PLLA: 65.7 ± 2.1 vs. $50 \pm 3.4\%$, $p < .01$; PLLA-DM: 61.1 ± 0.6 vs. $50 \pm 0.9\%$, $p < .01$; and PLLA-DMcx43: $64.6 \pm 2.9\%$ vs., $50.4 \pm 3.2\%$, $p < .01$). However, these early reductions in EF% were significantly lower in the three

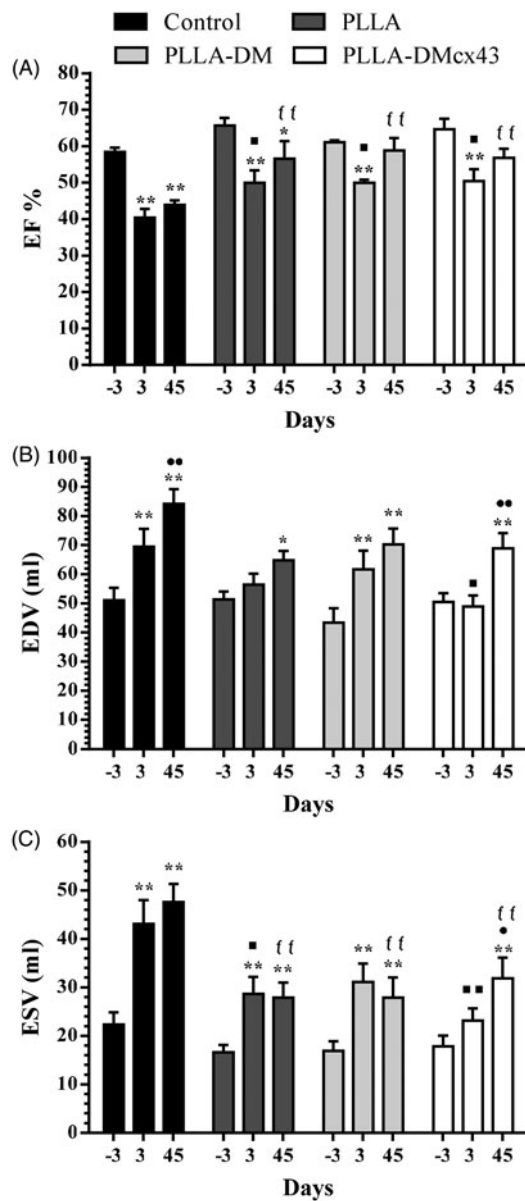


Figure 2. Left ventricular function. (A) Percent ejection fraction (EF%). (B) End-diastolic volume (EDV). (C) End-systolic volumes (ESV). * $p < .05$ and ** $p < .01$ vs. day 3 of the same group; • $p < .05$ and •• $p < .01$ vs. day 3 of the same group; ■ $p < .05$ and ■■ $p < .01$ vs. day 3 of the control group; ff $p < .01$ vs. day 45 of the control group. (mean \pm SEM, two-way ANOVA, Bonferroni). PLLA: poly(l)lactic acid (PLLA) scaffold devoid of cells; PLLA-DM: PLLA scaffold seeded with diaphragmatic myoblasts (DM); PLLA-DMcx43: PLLA scaffold seeded with DM overexpressing connexin-43 (cx43).

treated groups (PLLA, PLLA-DM and PLLA-DMcx43) than in the control group ($p < .05$).

At 45 d post-AMI, the three groups with PLLA scaffolds reached higher EF% values than the control group (control: $43.9 \pm 1.1\%$; PLLA: $56.6 \pm 4.8\%$; PLLA-DM: $58.9 \pm 3.4\%$ and PLLA-DMcx43: $56.9 \pm 2.4\%$; all $p < .01$ vs. control). However, paired analysis revealed that only the two groups with cells seeded on PLLA recovered baseline EF% values (PLLA-DM: $58.9 \pm 3.4\%$ vs. $61.1 \pm 0.6\%$, $p = \text{NS}$; and PLLA-DMcx43: $56.9 \pm 2.4\%$ vs. $64.6 \pm 2.9\%$, $p = \text{NS}$).

EDV was similar in all groups at baseline (control: 51.1 ± 4.3 ml, PLLA: 51.4 ± 2.8 ml; PLLA-DM: 43.4 ± 5 ml, PLLA-DMcx43: 50.4 ± 3.1 ml; $p = \text{NS}$) and increased significantly over time, reaching similar values at end follow-up (control:

84.2 ± 5.03 ml; PLLA: 64.8 ± 3.3 ml; PLLA-DM: 70.3 ± 5.5 ml and PLLA-DMcx43: 68.9 ± 5.4 ml, $p = \text{NS}$), indicating comparable levels of LV remodeling in all groups (Figure 2(B)).

Baseline ESV was similar among groups and increased significantly at 3 d post-AMI in control (43.1 ± 4.9 vs. 22.4 ± 2.5 ml, $p < .01$), PLLA (28.7 ± 3.5 vs. 16.7 ± 1.5 ml, $p < .01$) and PLLA-DM (31.1 ± 3.8 vs. 16.9 ± 2.0 ml, $p < .01$) but not in PLLA-DMcx43 (23.2 ± 2.5 vs. 17.8 ± 2.3 ml, $p = \text{NS}$). Furthermore, the 3 d post-AMI value in PLLA-DMcx43 was significantly lower than that of the control group ($p < .01$). Finally, at 45 d, all groups reached significantly higher values than at baseline (control: 47.6 ± 3.7 ml, $p < .01$; PLLA: 27.9 ± 3.1 ml, $p < .01$; PLLA-DM: 27.9 ± 4.2 ml, $p < .01$ y PLLA-DMcx43: 31.9 ± 4.2 ml, $p < .01$). Interestingly, PLLA, PLLA-DM and PLLA-DMcx43 groups reached statistically similar ESV values but significantly lower than the control group, suggesting less contractile deterioration of the LV afforded by the PLLA scaffold (Figure 2(C)).

Fibrosis

Figure 3(B) shows percent fibrotic tissue in the infarct region and its adjacent normoperfused region at end follow-up. In the infarct area, percent fibrosis in PLLA-DMcx43 group ($58.7 \pm 8.0\%$) was significantly lower than in control ($93.9 \pm 3.0\%$, $p < .01$) and PLLA-DM ($83.3 \pm 8.7\%$, $p < .05$) and also lower (though not significantly) than in PLLA ($80.8 \pm 7.2\%$, $p = \text{NS}$). In the peri-infarct region, no significant differences among groups were observed. However, the PLLA-DMcx43 group tended to have less fibrosis (control: $26.4 \pm 4.3\%$; PLLA: $37.7 \pm 4.8\%$; PLLA-DM: $30.1 \pm 4.9\%$; PLLA-DMcx43: $13.1 \pm 5.6\%$; $p = \text{NS}$).

Representative Masson's trichrome-stained slices of all groups are shown in Figure 3(B). Interestingly in control animals, the limit between healthy and damaged myocardium was sharp and almost perpendicular to the endocardium while the three groups with PLLA (but mainly PLLA-DMcx43 group), showed irregular and diffuse limits with healthy tissue invading the scar.

Persistence of PLLA scaffolds

Epicardial regions with underlying infarction were stained with H/E (Figure 3(C)). Light microscopy showed in all groups the characteristic cellular and extracellular matrix disarray of myocardial infarction. However, sections of PLLA groups showed remains of refringent material surrounded by granuloma with the presence of epithelioid cells. Giant multinucleated cells juxtaposed with the surface of the foreign body responsible for phagocytosing and degrading the biopolymer were also observed. These images reveal that PLLA scaffolds remained engrafted and were not completely reabsorbed after 45 d.

Microvascular density

Capillary density (Figure 4(A)) was significantly higher in PLLA-DMcx43 group (2003 ± 174 cap/mm²) than in control

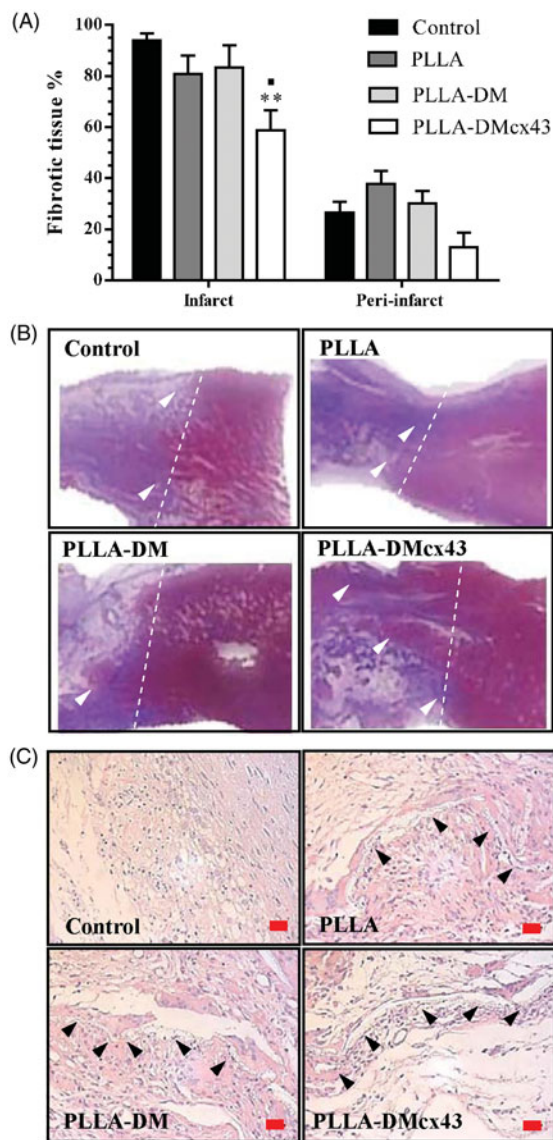


Figure 3. Histological analysis. (A) Percent fibrotic tissue in the infarct and peri-infarct regions. * $p < .05$ vs. control group and $\blacksquare p < .05$ vs. PLLA-DM group (mean \pm SEM, one-way ANOVA, Bonferroni). (B) Representative slices of the infarct border of an animal of each group stained with Masson's trichrome, showing vital (red) and fibrotic (blue) tissue at each side of a line drawn perpendicular to the endocardial limit of the infarct. In the animal treated with PLLA-DMcx43, vital myocardium penetrating the infarct can be observed (arrow heads). (C) Representative slices of epicardial regions with underlying infarction stained with hematoxylin/eosin. Arrow heads indicate the presence of the biomaterial in animals treated with the PLLA scaffold at 45 days post-implant. Bars: 20 μ m. PLLA: poly(l)lactic acid (PLLA) scaffold devoid of cells; PLLA-DM: PLLA scaffold seeded with diaphragmatic myoblasts (DM); PLLA-DMcx43: PLLA scaffold seeded with DM overexpressing connexin-43 (cx43).

and PLLA groups (control: 1184 ± 117 cap/mm²; PLLA: 1241 ± 130 cap/mm²; both $p < .05$) and also higher, though not significantly, than PLLA-DM group (1580 ± 211 cap/mm²; $p = NS$). Arteriolar density (Figure 4(B)) was similar in all groups (control: 17.2 ± 3 art/mm²; PLLA: 14.4 ± 4.5 art/mm²; PLLA-DM: 14.4 ± 5.3 art/mm²; PLLA-DMcx43: 17.3 ± 4.3 art/mm², $p = NS$). Figure 4(C) and (D) show representative images of capillary and arteriolar densities at 45 d post-treatment.

Gene expression at 45 days

Figure 4(E) illustrates gene expression at end follow-up. VEGF mRNA levels were significantly higher in all 3 treatment groups than in control (control: 1.00 ± 0.08 , PLLA: 1.55 ± 0.03 , PLLA-DM: 1.56 ± 0.07 , and PLLA-DMcx43: 1.61 ± 0.07 ; all $p < .01$ vs. control). A similar pattern was observed in PGF mRNA levels (control: 1.00 ± 0.05 , PLLA: 1.86 ± 0.1 ; PLLA-DM: 1.71 ± 0.2 ; PLLA-DMcx43: 1.76 ± 0.2 ; all $p < .01$ vs. control). Angiogenin expression showed a tendency to be higher in all three treatment groups (PLLA: 1.36 ± 0.06 ; PLLA-DM: 1.11 ± 0.2 ; PLLA-DMcx43: 1.36 ± 0.2) than in control (1.00 ± 0.1 , $p = NS$). As regards expression of Nkx 2.5, GATA-4 and C-Kit, their mRNA levels were higher in all 3 treatment groups than in control (Nkx2.5: control: 1.00 ± 0.09 ; PLLA: 1.59 ± 0.05 , PLLA-DM: 1.46 ± 0.1 , PLLA-DMcx43: 1.73 ± 0.09 , all $p < .05$ vs. control; GATA-4: control: 1.00 ± 0.07 , PLLA: 1.69 ± 0.05 , PLLA-DM: 1.56 ± 0.1 , PLLA-DMcx43: 1.65 ± 0.09 , all $p < .01$ vs. control; C-Kit: control: 1.00 ± 0.06 , PLLA: 1.41 ± 0.03 , PLLA-DM: 1.45 ± 0.05 , PLLA-DMcx43: 1.31 ± 0.07 , all $p < .01$ vs. control).

Discussion

The implant of adult stem cells is one of the approaches that more interest has aroused in the field of tissue regeneration. The results of this strategy not only depend on the type and origin of the cells used. Several authors have explained how cell migration, differential stimulation in cell signaling pathways, cell growth and other related functions are intimately associated with chemistry, structure and mechanical properties of the substrate [13–18]. Thus, implanting cellular sheets with a defined architecture and support may help achieving more effective cardioprotection. Hence, we have previously shown that PLLA scaffolds with aligned microfibers allow alignment of the cells used in the present study, mimicking muscle cell topography. As PLLA, it is a FDA-approved synthetic polyester used in biomedical applications, such as bioresorbable implants and tissue engineering [19,20]

Recently, it has been reported that its use in the form of scaffolds may serve as a delivery system for specific molecules or cells [21,22].

Another aspect to be taken into account is promoting inter-cell connectivity to favour propagation of the action potentials. It has been shown that the direct intramyocardial injection of skeletal myoblasts modified to overexpress cx43, significantly improves post-AMI LV function and prevents arrhythmias [23,24].

In our case, in addition to overexpression of cx43, inter-cell connectivity was likely favoured by the alignment of the cells, which augmented the contact surface between them. In fact, it has been shown that growing skeletal myoblasts over aligned and non-aligned scaffolds results in a differential stimulation of cellular signaling pathways among cells [13].

To assess the effect of aligned diaphragmatic myoblasts overexpressing cx43 seeded on PLLA scaffolds on infarct size and LV function, we used an ovine model of AMI. The use of a large mammal with biological features such as life span, gestation time, heart size and hemodynamics, more similar to the human than those of laboratory rodents, allows a higher

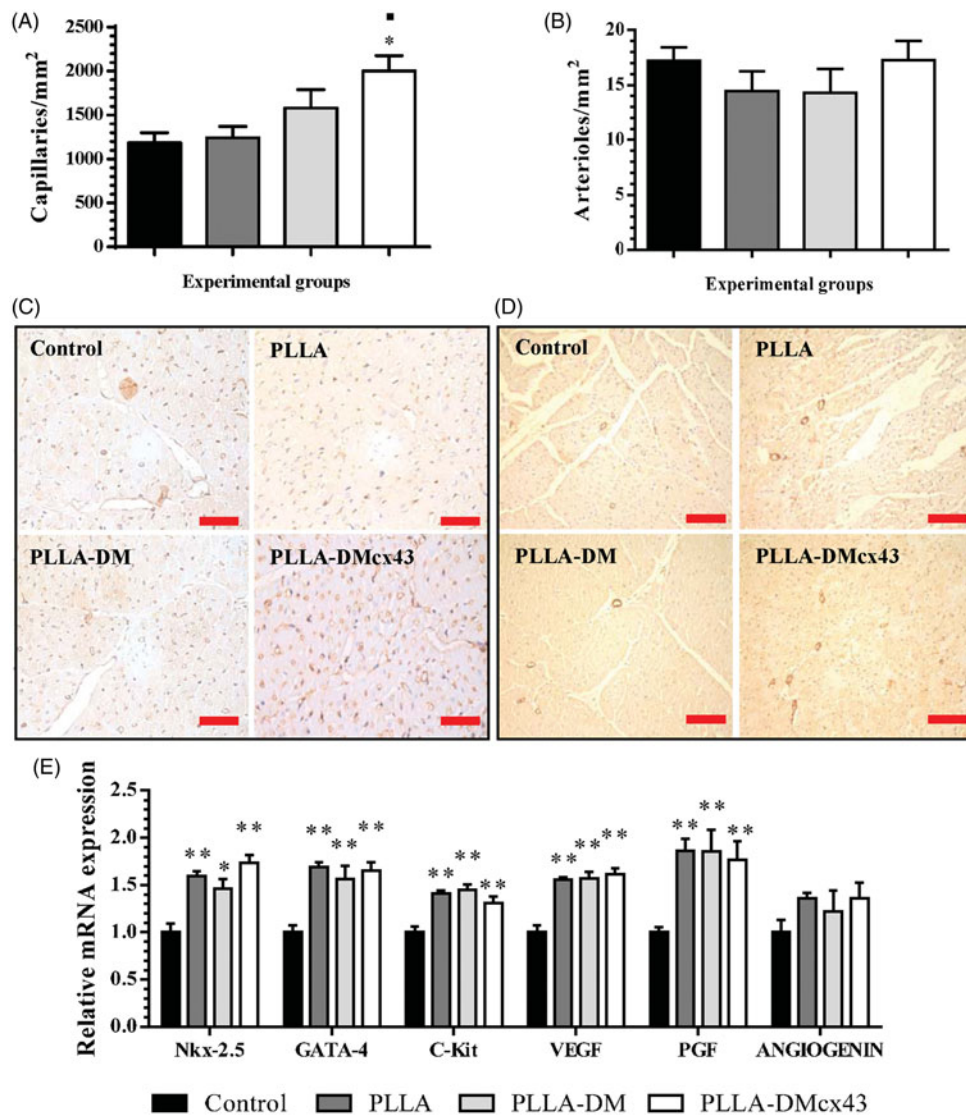


Figure 4. Microvascular density and gene expression. Capillary (A) and arteriolar (B) densities. * $p < .05$ vs. control group and ■ $p < .05$ vs. PLLA group. (C,D) Representative images of capillaries stained with a biotinylated lectin (bars: 50 μm) and arterioles stained with an antibody against smooth muscle actin (bars: 100 μm), respectively. (E) Relative expression of angiogenic and cardiomyogenic genes by real-time PCR. * $p < .05$ and ** $p < .01$ vs. control group. (mean ± SEM, one-way ANOVA, Bonferroni). PLLA: poly(l)lactic acid (PLLA) scaffold devoid of cells; PLLA-DM: PLLA scaffold seeded with diaphragmatic myoblasts (DM); PLLA-DMcx43: PLLA scaffold seeded with DM overexpressing connexin-43 (cx43).

level of reliability when extrapolating results to man. Although the large mammal more commonly employed in studies of cardiac regeneration is the pig, sheep have two significant advantages: first, while porcine cardiomyocytes have up to 32 nuclei [25], ovine cardiomyocytes have 1–4 nuclei, resembling human ones; and second, while 40–45 kg young adult sheep, as those used in the present study, may change their body weight by 5–10% in 45 d, pigs with the same initial weight can duplicate it and this, in turn, may lead to errors when interpreting changes in cardiac dimensions. Although allowing a more reliable extrapolation of results to the human, it is important to note that the animal model used does not accurately mimic the clinical setting, on account that we studied young adult animals lacking all risk factors of ischemic heart disease.

Given that, sheep coronary anatomy displays significant inter-individual variability [26], we visually inspected the LAD artery distribution in each animal and decided which

branches to ligate to induce an infarct spanning 15–20% of the LV and so minimize dispersion in initial infarct sizes. In effect, inter-group comparisons showed that the volume of infarcted myocardium soon after occlusion did not differ among groups.

CMR, a method that allows comparing infarct size on a paired basis, showed that the application of PLLA sheets with DMcx43 cells on the infarct and its adjacent region reduced the scar by ~25% after 45 d follow-up, an effect not observed in the other groups. Despite the observed effect, we could not detect DMcx43 at end follow-up. Although we have not tracked the cells at earlier time points, this would have been interesting not only to assess whether they had been present in the myocardium, but also if the expression of cx43 has differential effects on cell survival or engraftment.

As this group displayed the highest capillary density, it is sound to assume that, at least in part, enhanced perfusion to

the ischemic myocardium protected it from evolving into necrosis. Although VEGF, a paradigmatic angiogenic factor, was overexpressed to a similar extent in all three treated groups, it should be noted that skeletal myoblasts secrete numerous other growth factors and cytokines involved in vasculogenesis, as follistatin-like 1, FGF-2 and IGF-1 [27], which may have contributed to enhanced capillary growth in the groups receiving cells. In fact, the group receiving non transduced cells showed a tendency to augmented capillary density, though not significantly different from control. However, increased angiogenesis does not necessarily imply improved perfusion. It would have been interesting to assess myocardial perfusion through Single Photon Emission Computed Tomography (SPECT) scans. Still, the presence of erythrocytes within the capillaries strongly suggests that the neoformed vessels were functional.

The increased expression of genes involved in recruitment and differentiation of cardiomyocyte precursors indicates that cardiomyogenesis occurred. GATA-4 encodes a member of the GATA family of zinc-finger transcription factors known to regulate genes involved in embryogenesis and myocardial differentiation and function [28]. C-Kit encodes a tyrosine kinase receptor essential for proliferation, survival and migration of several stem cell types, including adult cardiac stem cells [29] and Nkx 2.5 gene encodes a homeobox-containing transcription factors that intervene in processes such as heart development [30]. Increased gene expression levels were observed in all treated groups, this suggests that is was the biomaterial, rather than the cells, which induced this effect [31]. Consistently, global LV function, as indicated by EF%, recovered to a similar extent in the three treated groups. This recovery stemmed mainly from improved contractile performance, as indicated by a significantly lower ESV than in control animals, which, in turn, is consistent with cardiomyogenesis. Besides, all three treatments limited LV remodeling to the same degree, as indicated by similar EDV values at end of follow-up. In other words, the mere presence of the PLLA scaffold induced LV function improvement, independently from infarct size reduction, an effect that only occurred in the PLLA-DMcx43 group. This is consistent with reports showing that post-AMI early mechanical support due to the presence of acellular biomaterials improves cardiac dynamics [22,32,33]. However, taking into account that at 45 d the scaffold was still present, we cannot rule out that at longer follow-up times, when the biomaterial is completely reabsorbed, the effect on LV function of reducing infarct size may become apparent.

Finally, quantification of fibrotic tissue showed that in the PLLA-DMcx43 group the tissue stained pink (vital myocardium) surrounding the infarct advanced into de scar (Figure 3(A) and (B)), this supporting the assumption that the observed increase in angiogenesis in the peri-infarct zone contributed to salvage jeopardized myocardium and hence reduce infarct size in this group. Whether or not recruitment and proliferation of cardiomyocyte precursors participated in this phenomenon cannot be asserted from our experiments.

In conclusion, in a sheep model of AMI at 45 d follow-up, the implant of PLLA sheets seeded with DM overexpressing cx43 induces angiogenesis, decreases fibrosis in the infarct

border and reduces infarct size. Global ventricular function, and the expression of genes associated with cardiac repair processes improve regardless of the presence of cells in the scaffold, indicating that these effects are induced by the biomaterial. The approach used in this study, combining cardio-regenerative strategies that are usually used individually is feasible, does not entail technical complications and exhibits a good level of safety, allowing to reduce infarct size in a large mammal. Further studies at longer follow-up periods are needed to assess whether the observed lack of relationship between infarct size reduction and differential effects on cardiac performance is still present in the long-term, when the biomaterial has been completely reabsorbed.

Acknowledgements

The authors thank veterinarians María Inés Besansón and Pedro Iguain for anesthetic management and animal house assistants Juan C. Mansilla, Osvaldo Sosa, and Juan Ocampo for care of the animals. We also thank Rosana Valverdi, Julio Martínez and Fabián Gauna for technical help.

Disclosure statement

No potential conflict of interest was reported by the authors.

Funding

This work was supported by the National Agency for the Promotion of Science and Technology (ANPCyT) of Argentina under Grant PICT 2011–1181 and 2012–0224; the René Barón Foundation of Argentina; the Florencio Fiorini Foundation of Argentina; and the National Scientific and Technical Research Council (CONICET) of Argentina.

ORCID

Carlos Sebastián Giménez  <http://orcid.org/0000-0001-8485-8343>

References

- [1] World Health Organization. Global status report on noncommunicable diseases [cited 2018 May 17] 2014. Geneva, Switzerland Available from <http://www.who.int/nmh/publications/ncd-status-report-2014/en/>.
- [2] Tiyyagura SR, Pinney SP. Left ventricular remodeling after myocardial infarction: past, present, and future. *Mt Sinai J Med.* 2006;73:840–851.
- [3] Lenderink T, Simoons ML, Van Es GA, et al. Benefit of thrombolytic therapy is sustained throughout five years and is related to TIMI perfusion grade 3 but not grade 2 flow at discharge. The European Cooperative Study Group. *Circulation.* 1995; 92:1110–1116.
- [4] Pfeffer JM, Pfeffer MA, Fletcher PJ, et al. Progressive ventricular remodeling in rat with myocardial infarction. *Am J Physiol.* 1991;260:H1406–H1414.
- [5] Cohn JN. Post-MI remodeling. *Clin Cardiol.* 1993;16:II21–II24.
- [6] Alkan M, Madanieh R, Shah NN, et al. Regenerative stem cell therapy optimization via tissue engineering in heart failure with reduced ejection fraction. *Cardiovasc Eng Tech.* 2017;8:515–526.
- [7] Menasche P. Skeletal muscle satellite cell transplantation. *Cardiovasc Res.* 2003;58:351–357.

- [8] Perez-Illarbe M, Agbulut O, Pelacho B, et al. Characterization of the paracrine effects of human skeletal myoblasts transplanted in infarcted myocardium. *Eur J Heart Fail.* 2008;10:1065–1072.
- [9] Baroffio A, Bochaton-Piallat ML, Gabbiani G, et al. Heterogeneity in the progeny of single human muscle satellite cells. *Differentiation.* 1995;59:259–268.
- [10] Redshaw Z, McOrist S, Loughna P. Muscle origin of porcine satellite cells affects in vitro differentiation potential. *Cell Biochem Funct.* 2010;28:403–411.
- [11] Giménez CS, Locatelli P, Montini Ballarin F, et al. Aligned ovine diaphragmatic myoblasts overexpressing human connexin-43 seeded on poly (L-lactic acid) scaffolds for potential use in cardiac regeneration. *Cytotechnology.* 2018;70:651–664.
- [12] Locatelli P, Olea FD, De Lorenzi A, et al. Reference values for echocardiographic parameters and indexes of left ventricular function in healthy, young adult sheep used in translational research: comparison with standardized values in humans. *Int J Clin Exp Med.* 2011;4:258–264.
- [13] McClure MJ, Clark NM, Hyzy SL, et al. Role of integrin $\alpha 7 \beta 1$ signaling in myoblast differentiation on aligned polydioxanone scaffolds. *Acta Biomater.* 2016;39:44–54.
- [14] Abbott A. Cell culture: biology's new dimension. *Nature.* 2003;424:870–872.
- [15] Kenar H, Kose GT, Hasirci V. Design of a 3D aligned myocardial tissue construct from biodegradable polyesters. *J Mater Sci.* 2010;21:989–997.
- [16] Jia L, Prabhakaran MP, Qin X, et al. Guiding the orientation of smooth muscle cells on random and aligned polyurethane/collagen nanofibers. *J Biomater Appl.* 2014;29:364–377.
- [17] Díaz-Gómez L, Ballarin FM, Abraham GA, et al. Random and aligned PLLA: PRGF electrospun scaffolds for regenerative medicine. *J Appl Polym Sci.* 2015;132:n/a. Available from <http://onlinelibrary.wiley.com/doi/10.1002/app.41372/abstract>.
- [18] Shalumon KT, Deepthi S, Anupama MS, et al. Fabrication of poly (l-lactic acid)/gelatin composite tubular scaffolds for vascular tissue engineering. *Int J Biol Macromol.* 2015;72:1048–1055.
- [19] Gupta B, Revagade N, Hilborn J. Poly (lactic acid) fiber: an overview. *Prog Polym Sci.* 2007;32:455–482.
- [20] Lopes MS, Jardim AL, Filho RM. Poly (Lactic Acid) production for tissue engineering applications. *Procedia Eng.* 2012;42:1402–1413.
- [21] Liu Q, Tian S, Zhao C, et al. Porous nanofibrous poly(L-lactic acid) scaffolds supporting cardiovascular progenitor cells for cardiac tissue engineering. *Acta Biomater.* 2015;26:105–114.
- [22] Spadaccio C, Nappi F, De Marco F, et al. Implantation of a poly-l-lactide gcsf-functionalized scaffold in a model of chronic myocardial infarction. *J F Cardiovasc Trans Res.* 2017;10:47–65.
- [23] Kolanowski TJ, Rozwadowska N, Malcher A, et al. In vitro and in vivo characteristics of connexin 43-modified human skeletal myoblasts as candidates for prospective stem cell therapy for the failing heart. *Int J Cardiol.* 2014;173:55–64.
- [24] Abraham MR, Henrikson CA, Tung L, et al. Antiarrhythmic engineering of skeletal myoblasts for cardiac transplantation. *Circ Res.* 2005;97:159–167.
- [25] Gräbner W, Pfitzer P. Number of nuclei in isolated myocardial cells of pigs. *Virchows Arch B Cell Pathol.* 1974;15:279–294.
- [26] Locatelli P, Olea FD, Mendiz O, et al. An ovine model of postinfarction dilated cardiomyopathy in animals with highly variable coronary anatomy. *Illar J.* 2011;52:E16–E21.
- [27] Henningsen J, Rigbolt KT, Blagoev B, et al. Dynamics of the skeletal muscle secretome during myoblast differentiation. *Mol Cell Proteomics.* 2010;9:2482–2496.
- [28] Oka T, Maillet M, Watt AJ, et al. Cardiac-specific deletion of Gata4 reveals its requirement for hypertrophy, compensation, and myocyte viability. *Circ Res.* 2006;98:837–845.
- [29] Ellison GM, Vicinanza C, Smith AJ, et al. Adult c-kit(pos) cardiac stem cells are necessary and sufficient for functional cardiac regeneration and repair. *Cell.* 2013;154:827–842.
- [30] Benson DW, Silberbach GM, Kavanaugh-McHugh A, et al. Mutations in the cardiac transcription factor NKX2.5 affect diverse cardiac developmental pathways. *J Clin Invest.* 1999;104:1567–1573.
- [31] Domingos AL, Garcia SB, Bessa Junior J, et al. Expression of VEGF and collagen using a latex biomembrane as bladder replacement in rabbits. *Int Braz J Urol.* 2012;38:536–543.
- [32] Pilla JJ, Blom AS, Gorman JH, et al. Early postinfarction ventricular restraint improves borderzone wall thickening dynamics during remodeling. *Ann Thorac Surg.* 2005;80:2257–2262.
- [33] Ifkovits JL, Tous E, Minakawa M, et al. Injectable hydrogel properties influence infarct expansion and extent of postinfarction left ventricular remodeling in an ovine model. *Proc Natl Acad Sci USA.* 2010;107:11507–11512.